

Experimental study of the pressure drops during Condensation of R134a in inclined tubes at different saturation temperatures

Adekunle O. Adelaja ^{*}, Jaco Dirker ^{**}, Josua P. Meyer ^{*}**

Department of Mechanical and Aeronautical Engineering, University of Pretoria, Private Bag X20, Hatfield 0028, Pretoria, South Africa.

**Corresponding author:*

Email: josua.meyer@up.ac.za

Phone: +27 12 420 3104,

***Alternative Corresponding Author:*

Email: jaco.dirker@up.ac.za

Phone: +27 12 420 2465

****Alternative Corresponding Author:*

Email: kunle.adelaja@up.ac.za

Abstract

An experimental study of the pressure drops during the condensation of R134a in a smooth copper tube of inner diameter of 8.38 mm was carried out for vapour qualities ranging between 0.1 and 0.9, mass fluxes between 100 kg/m²s and 400 kg/m²s, and saturation temperatures between 30°C and 50°C. Inclination angles ranging from –90° (downward flow) to +90° (upward flow) were considered. The pressure drop was measured directly by means of calibrated differential pressure transducers connected to the inlet and the outlet of the test condenser. It was found that the pressure drop is significantly influenced by the inclination angle and saturation temperature. The void fraction and frictional pressure drop results also show that they are largely influenced by these parameters. While the highest and lowest measured pressure drops were obtained during the upward flow and downward flow respectively, the results obtained for the void fraction and the frictional pressure drop showed that the highest values were obtained during the downward flow while the lowest values were obtained during the horizontal and upward flows.

Keywords: pressure drop, frictional pressure gradient, inclined tubes; smooth tube; R134a

Nomenclature

g	gravitational acceleration (m/s ²)
G	mass flux (kg/m ² s)
$L_{\Delta P}$	distance between the pressure taps (m)
P	pressure (kPa)
$\Delta P_{T_{sat}}$	pressure difference between two saturation temperatures (kPa)
Q	heat transfer rate (W)
T	temperature (°C)

x vapour quality (-)

Greek symbols

β inclination angle (rad)

ε void fraction (-)

ρ density (kg/m³)

Subscripts

fric frictional

H₂O water

in inlet

l liquid

lines lines between pressure taps and transducer

m mean

meas measurement

mom momentum

out outlet

sat saturation

stat static

test test condenser

tp two-phase

v vapour

1. Introduction

Good heat exchanger design can contribute immensely to energy savings especially in the air conditioning and refrigeration industry, hydrocarbon processes, chemical plants, thermal plants and power plants. Design engineers are interested in both pressure drop and heat transfer performances. This is so because there is need to strike a balance between obtaining desirable low pressure drops to reduce pumping cost while maintaining the correct suction pressure downstream of the heat exchanger and the maximisation of the heat transfer per unit area. . In an attempt to achieve higher heat transfer coefficients through increased mass flow rates, higher pressure drops are attained resulting in higher pumping cost. Therefore, during the design and optimisation of phase change heat exchangers, the correct and precise estimation of the pressure drop in both the evaporator and condenser is paramount. The two-phase pressure drop between the inlet and outlet can be directly influenced by the saturation temperature. Also, there is an associated increase in pressure drop and heat transfer due to friction.

Several studies have been carried out on two-phase pressure drop [1-3]. Very few among these studies were done on pressure drop in inclined tubes [3], as the majority of the studies were on vertical and horizontal flows. Quiben and Thome [2] categorised the works done on predictions of pressure drop into three classes: empirical correlations, analytical models and phenomenological models. In their work, several studies were reviewed under these three classes. They further proposed flow pattern based models to predict frictional pressure drop. The earlier established correlations of Lockhard and Martinelli [4], Chisholm [5], Friedel [6], Gronnerud [7] and, Muller-Steinhagen and Heck [8] correlations were based on empirical relations which are easy to develop and often provide good accuracy due to the range of databases available for their development. Though, they were established for conventional

channels, they are also useful in predicting pressure drop in mini- and micro- channels. In their analytical approach, Spartz and Molta [9] used the works of Cavallini *et al.* [10] and Choi *et al.* [11] for their simulation. Their results showed that the heat transfer coefficient and pressure drop of R290 was 1.4 times and 2 times that of R410 respectively. Ghodbane [12] simulated a mobile air conditioning system using R290, RC270 and R600a as an alternative refrigerant to R134a. The heat transfer coefficient was calculated from Akers and Rosson's [13] correlation and the two-phase pressure drop was estimated from the Dukler [14] model. Results showed that the refrigerants considered had higher heat transfer coefficient but lower pressure drop compared with R134a.

Phenomenological models that are theoretically based and which take into account the interfacial structure resulting from the different flow regimes, have also been developed. Some of these models are by Bandel [15], Beattic [16] and Hart *et al.* [17]. Tribbe and Muller-Steinhagen [18] compared some of the leading two-phase frictional pressure drop correlations using several mixtures namely, air-water, air-oil and water-steam. They found that the empirical model of Muller-Steinhagen gave the best and most reliable result. In another comparison made by Ould-Didi *et al.* [19], it was discovered that the methods of Gronnerud [7] and Muller-Steinhagen and Heck [8] were the best followed by that of Friedel [6]. In a later comparison Quiben and Thome [2] showed that their model which was phenomenological predicted their experimental result better than the empirical model.

Several other studies were done on the effect of saturation temperature on either or both heat transfer coefficient and pressure drop. Among these is an earlier work of the current authors [20] on the effect of saturation temperature on the condensation heat transfer coefficient of R134a in an inclined 8.38 mm inner diameter copper tube. In this work, it was reported that

heat transfer coefficient decreased with saturation temperature. Patil and Sapali [21], in their experimental study of the condensation of R134a and R404A in both smooth and microfinned U-tubes, reported a decrease in frictional pressure drop with saturation temperature of up to 23.5% and 45.6% in the smooth and microfinned tube respectively. Similarly, Kim *et al.* [22] noted a decrease in pressure drop with an increase in saturation temperature for diabatic CO₂ flow at saturation temperatures of -25°C and -15°C in horizontal and vertical smooth and microfinned tubes of approximately 3.5 mm inner diameter. Cavallini *et al.* [23] likewise confirm the findings of earlier authors as regards to the relationship between heat transfer coefficient and pressure drop with saturation temperature. Works on the effect of saturation temperature on the heat transfer coefficient and pressure drop in inclined tubes are scarce in the open literature. As a follow-up on from our earlier work, this investigation involves the experimental investigation of the pressure drop in inclined tubes.

The aim of this study is to present the effect of the flow inclination, vapour quality and saturation temperature on the pressure drops in a smooth circular tube with an inner diameter of 8.38 mm during the convective condensation of R134a for vapour qualities of 10%, 25%, 50%, 75% and 90%, mass fluxes between 100 kg/m²s and 400 kg/m²s, inclination angles between -90° and +90° for saturation temperature between 30°C and 50°C. Experimentally measured pressure difference data over the heat exchanger test section is reworked into frictional pressure drop values by employing the recent drift flux model of Bhagwat and Ghajar [24] to obtain the void fraction.

2. Experimental Apparatus

The test facility used for the study was the same as for some previous investigations [20, 25-28]. In earlier works like these, comprehensive descriptions and explanations were made.

However, an overview is presented in this paper.

2.1. The Refrigerant Loop

The test rig consisted of a refrigerant loop operated on a vapour compression cycle, and two water loops (Fig. 1). The refrigerant loop consisted of two high-pressure lines (the test line and the bypass line) and a low-pressure line through which refrigerant R134a was pumped with the aid of a hermetically sealed scroll compressor with a nominal cooling load of 10 kW. Refrigerant flow in each of the high-pressure lines was controlled by electronic expansion valves (EEVs).

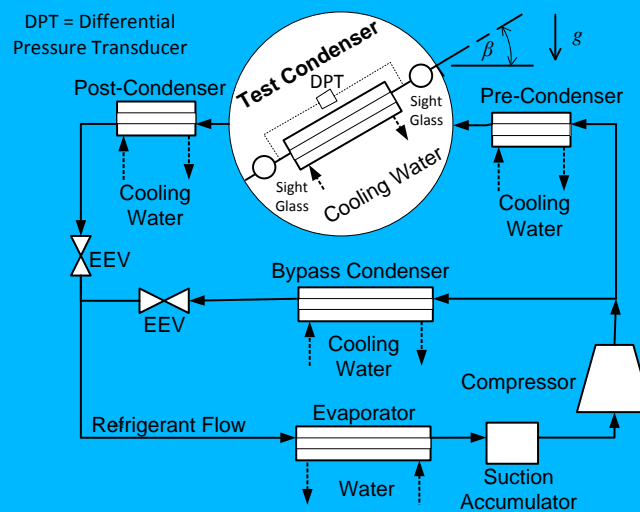


Fig. 1 Schematic diagram of the test rig.

The test line consisted of three condensers; the pre-condenser, test condenser and the post-condenser. The pre-condenser was used to regulate the inlet vapour quality into the test condenser where test measurements were carried out whereas the post-condenser was adjusted such that it ensured that there was complete condensation and subcooling, i.e. liquid refrigerant reached the EEV. Subcooling at the outlet of the post condenser was between 12.7°C and 34.7°C . The bypass condenser was used to control the mass flow rate, temperature and pressure of the refrigerant flowing through the test section. After the EEVs

the high-pressure lines united and led to the scroll compressor through the low-pressure line, which consisted of the evaporator and suction accumulator.

The test section was a copper tube-in-tube counter-flow heat exchanger in which the refrigerant flowed in the inner tube and water flowed in the annulus. It had a length of 1.488 m and had an inner-tube inside diameter of 8.38 mm and an outer tube inner diameter of 15.9 mm. The inner tube had a wall thickness of 0.6 mm (± 0.002 mm). To ensure that the flow through the test section was fully developed, a straight calming section, 50 diameters long, was situated at the entrance. At the inlet and outlet of the test section were sight glasses, which enabled flow visualisation and also served as insulators against axial heat conduction. A high-speed camera was installed at the outlet sight glass and was used to record and document the flow patterns. A uniform Phlox backlight was positioned against the sight glass to enable good colour fidelity due to its evenly distributed light-emitting diode (LED) illumination. Three pressure taps were connected between the sight glass and test section at both ends. Two of the pressure taps were connected to different Gem sensor pressure transducers for the measurement of the absolute pressure at both inlet and outlet sides of the section so that the absolute pressure recording used on each side was the average of two pressures. The third set of pressure taps was connected together to an FP 2000 Sensotec differential pressure transducer (DPT). See Fig. 1. Flexible hoses were used to connect the test section so that it could be inclined in any orientation between 90° upwards and 90° downwards. These pressure hoses were made of Nitrile, reinforced with two high tensile steel wire braids and covered with synthetic rubber. The hoses, which had inner diameters of 9.5 mm (3/8 inch) could withstand a pressure of up to 33 MPa and a temperature range of between -40°C and 100°C. These hoses were further insulated with polyethylene pipe insulation to reduce heat loss.

On the inner-tube's outer wall sets of four holes were drilled in seven equidistant stations such that at each station four, T-type thermocouples were soldered at the top, bottom and both sides of the tube. The 28 thermocouples spanned the heat exchanger length. The refrigerant temperatures were taken at the inlet and outlet of each condenser. At each location, three thermocouples were installed, one each on the top, bottom and side of the tube wall. All the thermocouples used were calibrated against a high-precision Pt-100 resistance temperature detector to an accuracy of 0.1°C. The consistency of the readings at these sections was checked between the saturation temperature obtained with the absolute pressure transducers and the saturation temperature acquired from the thermocouples. A Coriolis mass flow meter was used to measure the refrigerant flow rate in the test section.

2.2. The Water Loops

Cold and hot water were supplied respectively by a 50 kW heating and a 70 kW cooling dual-function heat pump. These were thermostatically controlled such that the cold and hot water temperatures were set to 10 °C – 15 °C and 25°C respectively. The hot and cold water were stored in two 5 000 litre insulated water tanks before supplied to the set-up. While hot water passed through the evaporator, the cold was supplied to the condensers. Water inlet- and outlet temperatures were obtained using three calibrated thermocouples at each station. Coriolis mass flow meters were used to measure the water flow rates. In order to determine the heat transfer rates in the pre- and post-condensers (which were needed for data processing), the water inlet and outlet temperatures as well as the water mass flow rates in these heat exchangers were also measured.

2.3 Data Acquisition

Data from the thermocouples, pressure transducers, and Coriolis flow meters were collected

by a computerised data acquisition (DAQ) system. The DAQ system consisted of a desktop computer on which was installed a LabVIEW program written to automatically acquire needed data, an analogue/digital interface card, shielded cable assembly, signal-conditioning extensions for instrumentation (SCXI), transducer multiplexers, terminal blocks, channel multiplexers and termination units. The program displayed all measurements, including both primary and secondary quantities, which were monitored until steady state was reached before data was captured. After steady state was reached, the different sensor signals were recorded continuously through the DAQ system for about a period of 5 minutes (121 points). In order to avoid noise measurement, the average of the points was used for the calculations of the fluid properties, heat transfer coefficient and other parameters of interest.

3. Data Reduction and Experimental Procedure

The refrigerant pressure was measured at the inlet of the test section by an analogue strain gauge transducer with an accuracy of ± 2 kPa for low mass fluxes ($100 \text{ kg/m}^2\text{s} - 200 \text{ kg/m}^2\text{s}$) and ± 12 kPa for high mass fluxes ($G > 300 \text{ kg/m}^2\text{s}$). The measured value when used with the condensation curve provided by REFPROP [29] gave the saturation temperature, which was verified by direct measurement. The difference in the two values was found to be less than 0.1°C at high mass fluxes ($400 \text{ kg/m}^2\text{s}$ and above) while a higher variation was observed at low mass fluxes. This might have been due to the non-uniformity of the flow patterns encountered for lower mass fluxes, particularly at the smooth-stratified, stratified-wavy and intermittent regions. The pressure drop across the test section was measured by a differential pressure transducer, which was calibrated to an accuracy of ± 0.05 kPa. The pressure measuring lines were heated between the pressure taps and the transducer such that the temperature was kept at about $5 - 10^\circ\text{C}$ above the saturation temperature so that only vapour was present. The heating elements used for this was controlled with the LabVIEW program.

The recorded pressure drop data collected at the test section was a combination of the measured and the line pressure drops. The pressure difference obtained at the differential pressure transducer was ΔP_{meas} while the difference in the pressure over the test section was

$$\Delta P_{test} = \Delta P_{meas} + \Delta P_{line} \quad (1)$$

where ΔP_{line} is the pressure difference in measuring line due to the gravitational effect expressed as

$$\Delta P_{line} = \rho_v g L_{\Delta P} \sin \beta \quad (2)$$

Where, ρ_v is the vapour density, g the acceleration due to gravity, $L_{\Delta P}$ is the distance between the pressure taps and β is the angle of inclination of the test section. β changes sign depending on the test section inclination. It is positive during upward inclination, zero for horizontal and negative during downward inclinations. A large number (more than 700) experimental pressure drops data points were collected. The conditions for the experiment are presented in Table 1.

The pressure difference in two-phase diabatic flow comprises of three components: the static, the momentum and the frictional pressure drops. This can be expressed as

$$\Delta P_{test} = \Delta P_{mom} + \Delta P_{stat} + \Delta P_{fric} \quad (3)$$

The momentum pressure drop ΔP_{mom} accounts for the difference in pressure due to the change in momentum resulting from the acceleration or deceleration of the fluid in the test

section. The static pressure drop ΔP_{stat} component results from an elevation difference between the inlet and the outlet due to the tube inclination angle. The frictional pressure drop component, ΔP_{fric} , comes from the effect of shear stress imparted by the wall of the flow channel on the fluid.

The static pressure drop in the test section can be expressed as:

$$\Delta P_{stat} = \rho_{tp} g L_{\Delta P} \sin \beta \quad (4)$$

where ρ_{tp} is the two-phase density of the fluid given as

$$\rho_{tp} = \rho_l(1 - \varepsilon) + \rho_v \varepsilon \quad (5)$$

with ρ_l being the density of the liquid phase and, ε being the void fraction. The momentum pressure drop is expressed as

$$\Delta P_{mom} = G^2 \left[\left(\frac{(1-x)^2}{\rho_l(1-\varepsilon)} + \frac{x^2}{\rho_v \varepsilon} \right)_{out} - \left(\frac{(1-x)^2}{\rho_l(1-\varepsilon)} + \frac{x^2}{\rho_v \varepsilon} \right)_{in} \right] \quad (6)$$

Void fraction is an important parameter which is needed to determine the static and momentum pressure differences in the test section. With the void fraction, other values such as the two-phase mixture viscosity, density and actual velocities can be obtained. Several experimental investigations have been conducted to measure the void fraction for various flow pattern regimes and fluids. Also, several models have been developed to correlate the

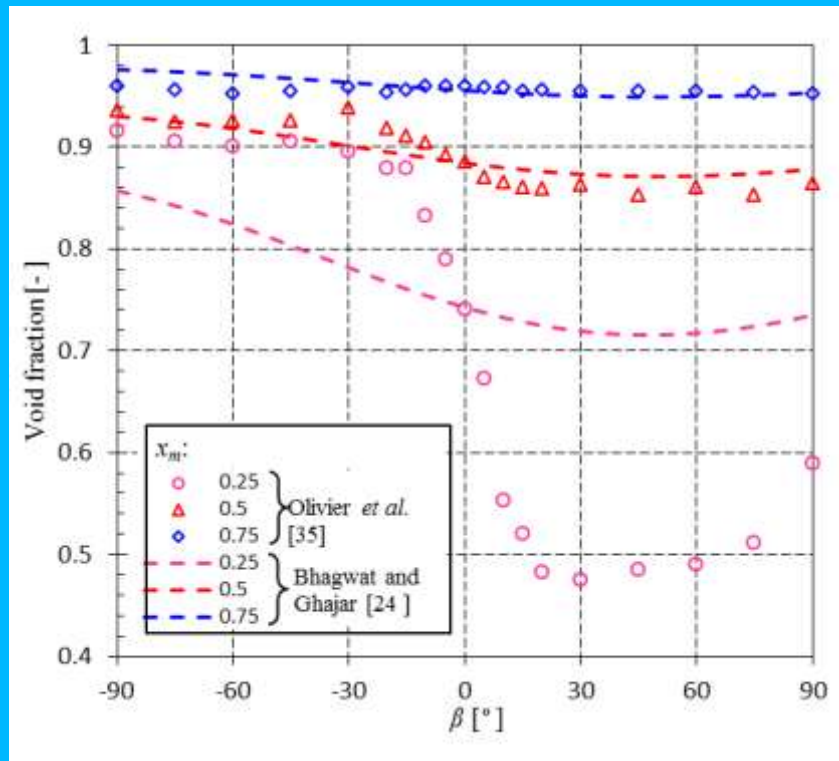


Fig. 2. Comparison of the predicted void fraction values with experimental values from Olivier et al [35] for $G = 100 \text{ kg/m}^2\text{s}$ and $T_{sat} = 40^\circ\text{C}$.

void fraction to measurable quantities such as the phase temperatures and the dimensions of the flow passage. Most correlations are, however, for horizontal and vertical tube orientations with only a limited number of studies focusing on inclined systems [30-34]. The available models can be categorized into three types: slip models; $k-\alpha$ models and drift flux model. For this study, the recent Bhagwat and Ghajar drift flux model [24], suitable for inclined passages is used to predict the void fraction in the test section. A comparison of the predicted void fraction using this model with experimental data from Olivier *et al.* [35] is shown in Fig. 2. It can be seen that relative good agreement exists between the predicted void fraction values and the measured void fractions at relatively high vapor qualities of 0.5 and 0.75. For these cases almost all void fraction data points are predicted correctly within a margin of 0.02. For a vapour quality of 0.25 an almost exact agreement exists for $\beta = 0^\circ$, however, the correlation seems to over-predict the void fractions for downward inclined flow and over-

predict the void fractions for upward inclined flow. Due to a lack of a better-performing correlation, all experimental data in this paper is process with the Bhagwat and Ghajar correlation.

4. Measured Pressure Drop Results

Pressure drop generally depends on the thermo-physical properties of the fluid, the mean vapour quality, the mass flux, the inclination angle and the saturation temperature. The uncertainty analysis was done for the measured pressure drop following the procedural analysis in Moffat [36]. This is necessary to evaluate the significance of the scatter on repeated trials. The differential pressure transducer had an accuracy of ± 0.05 kPa. This was taken as the bias uncertainty. The precision uncertainty was calculated from the data taken over 121 repeated points assuming 95% confidence level. The uncertainty varies between 0.05 kPa and 0.21 kPa where the highest was obtained for $G = 400$ kg/m²s, $T_{sat} = 30^\circ\text{C}$, $x_m = 0.25$ and $\beta = -60^\circ$.

4.1. Effect of the Inclination Angle on Measured Pressure Difference

Fig. 3 a - c indicate the effect of inclination angle on the measured pressure drop for different mass fluxes for a saturation temperature of 30°C for x_m of a) 0.25 b) 0.5 and c) 0.75. At a glance, the results show that the higher the x_m becomes, the higher the ΔP_{meas} is and the wider apart (larger) the difference in pressure drop is. Furthermore, as expected, it can be seen that the pressure difference generally increases with mass flux. From Fig. 3a (for $x_m = 0.25$) it can be seen that the ΔP_{meas} for $G = 100$ kg/m²s and 200 kg/m²s are relatively similar, except for the range of β between -10° and $+30^\circ$, and β greater than 60° . In the first range $G = 200$ kg/m²s has higher pressure differences, while for the second range the opposite is true. This can be attributed to higher liquid hold-up for these orientations for $G = 100$ kg/m²s. For $x_m = 0.5$ and

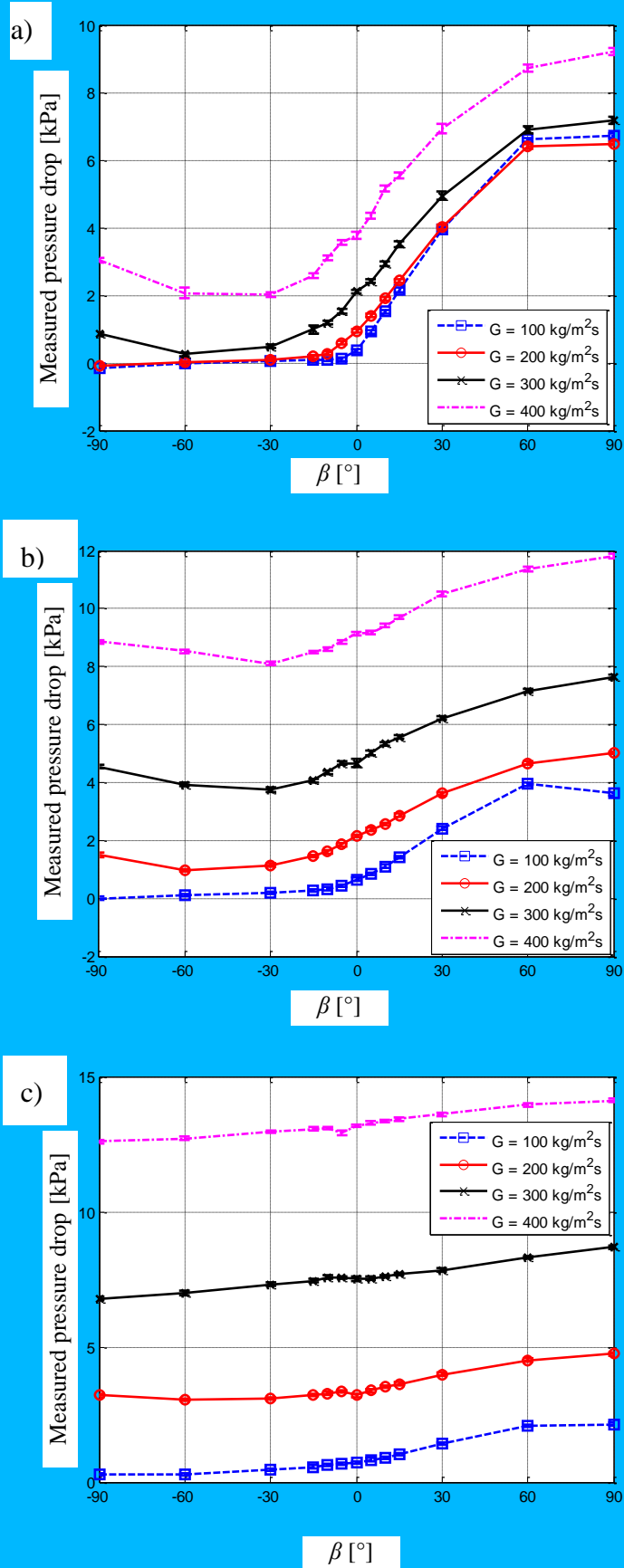


Fig. 3. Effect of inclination angle on pressure drop for different mass fluxes for a) $x_m = 0.25$, b) $x_m = 0.5$ and c) $x_m = 0.75$ for $T_{sat} = 30^\circ\text{C}$.

0.75, Figs. 3b and 3c reveal that there are clear differences in ΔP_{meas} for all mass flux cases and these differences increase with G and x_m . This can be ascribed to the fact that the flow becomes more annular as G increases. Fig. 4 presents the types of flow patterns encountered during the experiments while Fig. 5 shows the variation of the flow pattern with β at $x_m = 0.5$ and $T_{sat} = 30^\circ\text{C}$ for different G cases. The flow patterns observed for $G = 100 \text{ kg/m}^2\text{s}$ and $200 \text{ kg/m}^2\text{s}$ were basically stratified-wavy during the horizontal and slightly inclined orientations. As the tube orientation became vertical downward the flow transited from stratified-wavy to churn while close to vertical flow, it transited from stratified-wavy to intermittent. For upward flow, churn flow was predominant. For $G = 300 \text{ kg/m}^2\text{s}$ the flow was annular-wavy during the horizontal and slightly inclined orientations, and churn during the vertical upward and downward tube orientations. For $G = 400 \text{ kg/m}^2\text{s}$, the flow tended to be annular during all inclinations. By comparing the flow patterns in Fig. 5 with the pressure drop measurements in Fig.3b, it can be seen that when the flow was more annular, the higher the pressure drop was.

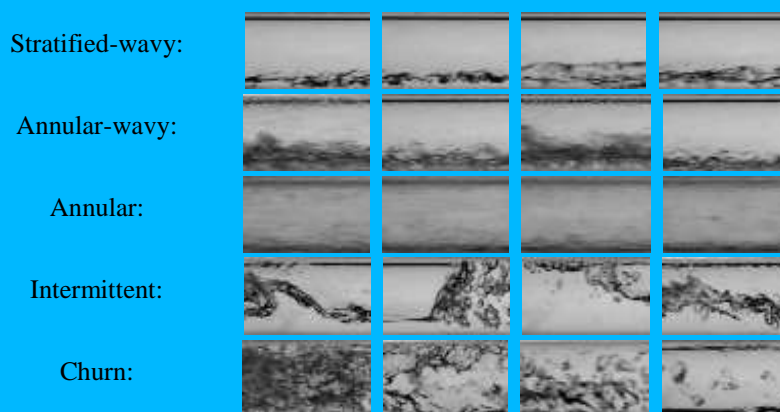


Fig. 4. The different types of flow patterns observed in this study.

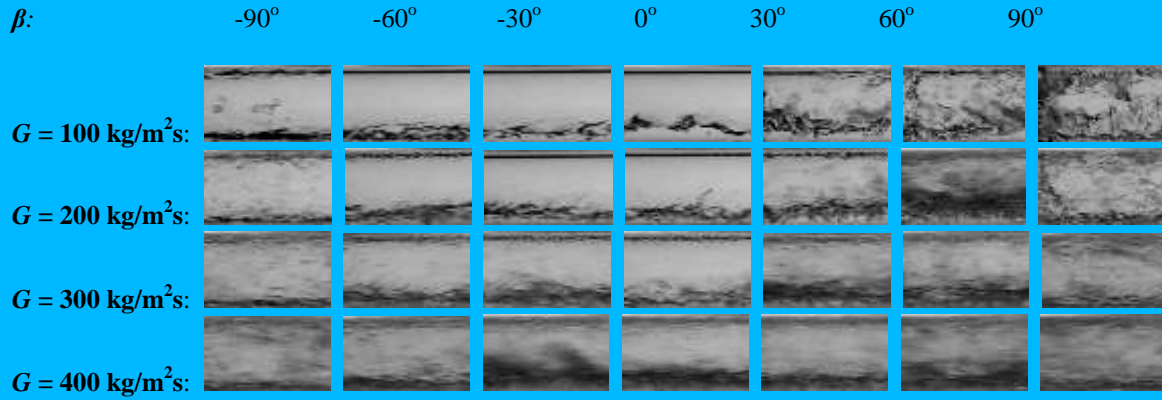


Fig. 5. Effect of the inclination angle on the flow pattern for different mass fluxes for $x_m = 0.5$ for $T_{sat} = 30^\circ\text{C}$.

4.2. Effect of Mean Vapour Quality on Measured Pressure Difference

Fig. 6 a – d show the effects of measured pressure drop as a function of the inclination angle (β) and mean vapour quality x_m for G of a) $100 \text{ kg/m}^2\text{s}$ b) $200 \text{ kg/m}^2\text{s}$ c) $300 \text{ kg/m}^2\text{s}$ and d) $400 \text{ kg/m}^2\text{s}$ for $T_{sat} = 30^\circ\text{C}$. During the data gathering stage, some heat transfer and pressure drop data for low mass fluxes ($< 100 \text{ kg/m}^2\text{s}$) were very difficult to collect due to instabilities in the recording and energy balance. For instance, at the saturation temperature of 30°C , the qualities of 0.25, 0.5 and 0.75 were obtained while at 50°C only the quality of 0.5 was obtained. This explains why some data points for $G = 100 \text{ kg/m}^2\text{s}$ are missing in Fig. 6 and later in Fig. 10 a and c. The results in Fig 6 show that the parameters (inclination angle, mean vapour quality and mass flux) have significant influences on the pressure drop. For high G and x_m , shear forces are dominant while the gravitational force is dominant in the low G , low x_m cases. For the same mass flux, decreasing x_m corresponds to increasing effective density which results in increasing static pressure component, hence resulting in higher the test pressure differences. Also, an increase in the inclination angle causes an increase in the static pressure effect which is responsible for higher pressure difference during upward flow as compared to downward and horizontal flow. The effect of the inclination angle is not significant for high mass flux and high vapour quality as can be seen in Fig. 6 c – d ($G = 300$

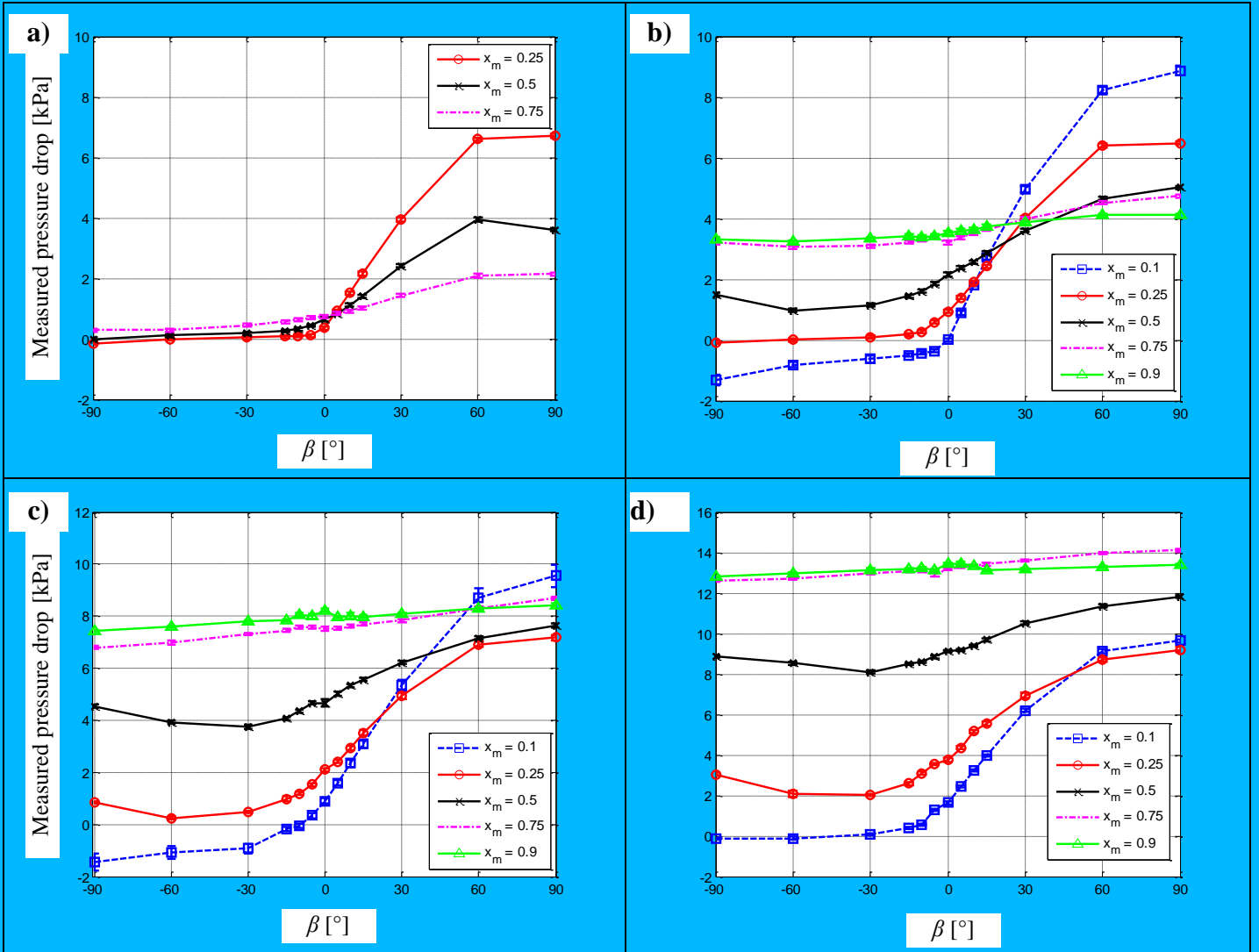


Fig. 6. Effect of inclination angle on pressure drop for different mean vapour quality for G of a) $100 \text{ kg/m}^2\text{s}$, b) $200 \text{ kg/m}^2\text{s}$, c) $300 \text{ kg/m}^2\text{s}$ and d) $400 \text{ kg/m}^2\text{s}$ for $T_{sat} = 30^\circ\text{C}$.

$\text{kg/m}^2\text{s}$, $x_m = 0.75$ and 0.9 ; $G = 400 \text{ kg/m}^2\text{s}$, $x_m = 0.75$ and 0.9). Furthermore, an increase in the mass flux results in an increase in the frictional component due to the increasing dominance of the shear force at the tube wall. A closer look shows that at low qualities ($x_m = 0.1$ for all G cases and $x_m = 0.25$ for $G = 100$ and $200 \text{ kg/m}^2\text{s}$) negative pressure differences were obtained during the downward flows. This phenomenon has also been reported by other researchers [37 - 44]. In their works, the phenomenon has been attributed to the presence of low liquid mass fluxes [37 - 40], instabilities in the flow which results into Taylor flow regime [41], slip flow at the vapour-liquid interface and liquid-wall interface termed “flow

reversal” [42 - 44].

Fig. 7 reveals the variation of the flow pattern with quality and inclination angle. Annular flow is mostly observed for qualities of 0.5, 0.75 and 0.9. For $x_m = 0.1$ and 0.25 flow patterns are intermittent for all inclination except for vertical downward and upward flows.

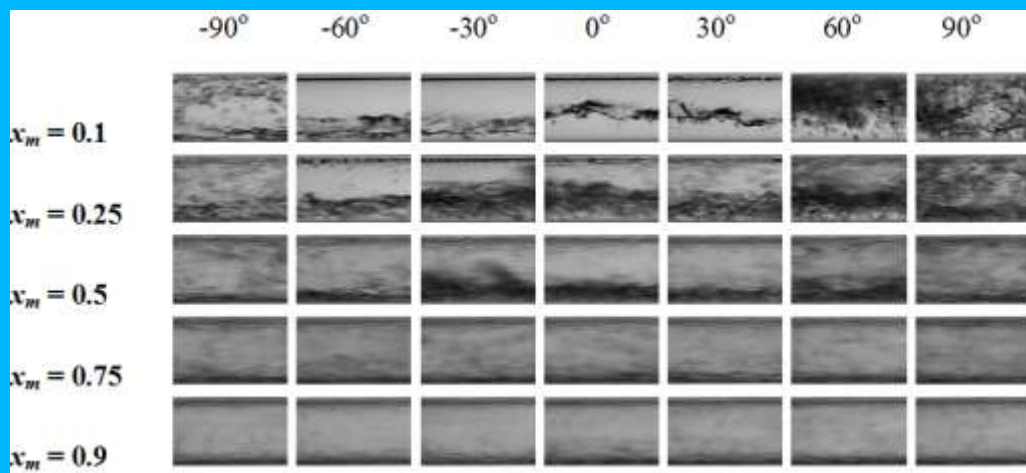


Fig. 7. Effect of inclination angle on the flow pattern for different mean vapour qualities for $G = 400 \text{ kg/m}^2\text{s}$ and $T_{sat} = 30^\circ\text{C}$.

4.3. Effect of Saturation Temperature on the Measured Pressure Difference

The impact of saturation temperature on pressure difference, particularly on inclined tubes, has been investigated by only a small number of researchers as highlighted in the literature review. In Fig. 8, the effect of saturation temperature on measured pressure drop is studied for different inclination angles for $G = 400 \text{ kg/m}^2\text{s}$ for a) $x_m = 0.25$, b) $x_m = 0.5$ and c) $x_m = 0.75$. The results show that ΔP_{meas} decreases as saturation temperature increases. It can also be seen that as x_m increases the ΔP_{meas} and difference in ΔP_{Tsat} increases. In addition, as x_m increases, the inclination effect becomes less dominant for all saturation the temperatures. The differences in the flow patterns for $G = 400 \text{ kg/m}^2\text{s}$, as shown in Fig. 9, are not distinctly

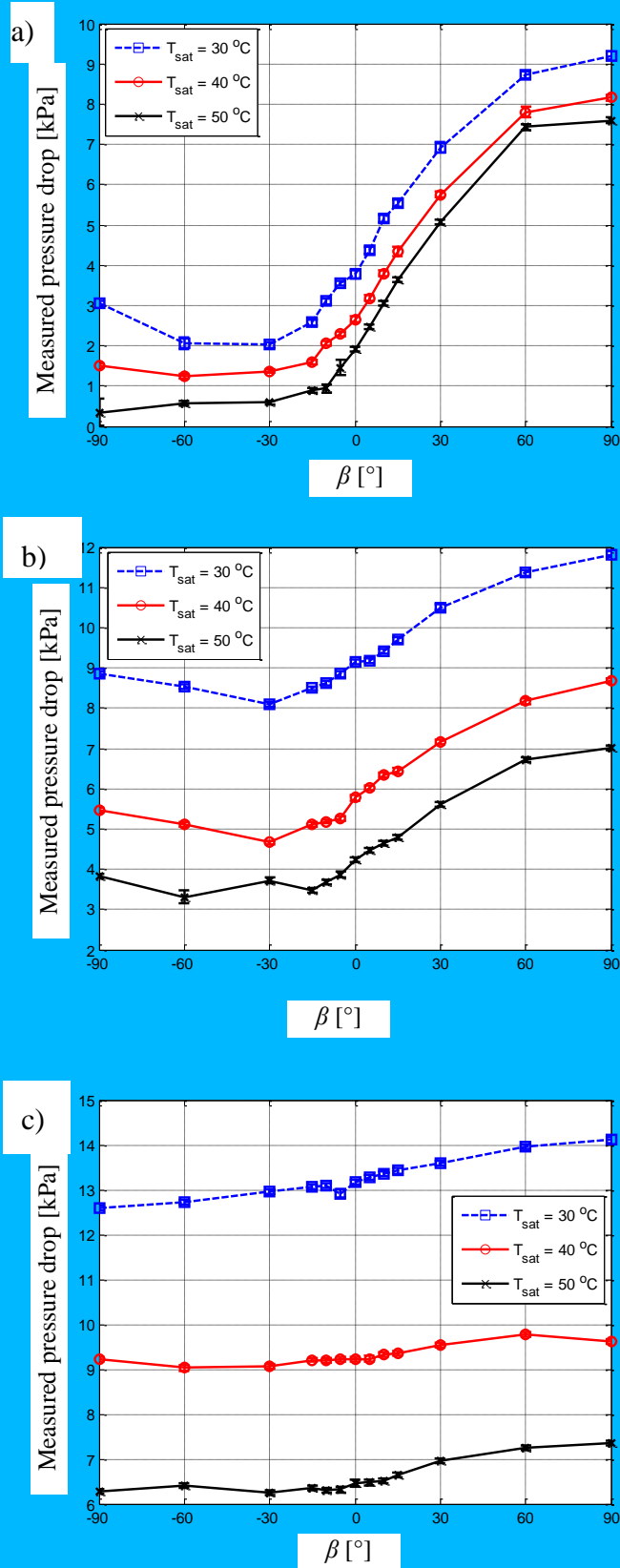


Fig. 8. Effect of inclination angle on pressure drop for different T_{sat} for $G = 400 \text{ kg/m}^2\text{s}$, a). $x_m = 0.25$, b). 0.5 and c). 0.75.

very different, especially between the flow patterns for $T_{sat} = 40^\circ\text{C}$ and $T_{sat} = 50^\circ\text{C}$ that were in the annular-wavy regime as compared with that of $T_{sat} = 30^\circ\text{C}$ that was more annular in nature. Consequently, as the saturation temperature is reduced, the flow becomes more annular resulting in higher the pressure differences.

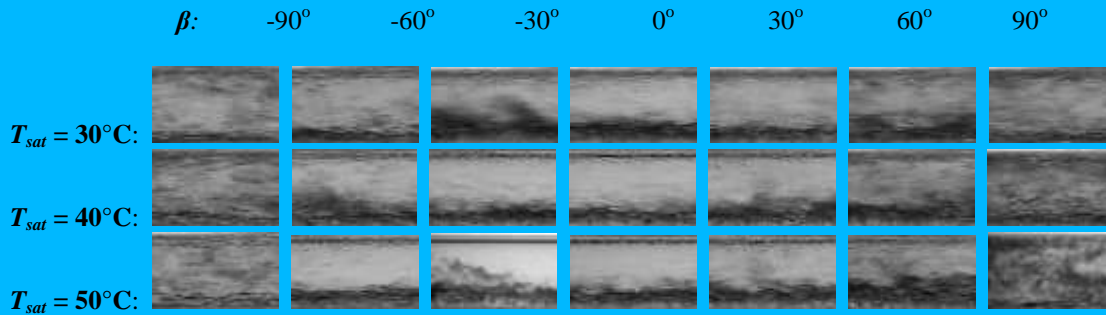


Fig. 9. Effect of inclination angle on the flow pattern for different saturation temperature for $x_m = 0.5$ and $G = 400 \text{ kg/m}^2\text{s}$.

The effect of G on the pressure difference for different saturation temperatures for $\beta = 0^\circ$ and a) $x_m = 0.25$, b) $x_m = 0.5$ and c) $x_m = 0.75$ is illustrated in Fig. 10. For this inclination the results reveal that ΔP_{meas} increases with G irrespective of x_m . Higher ΔP_{meas} corresponds to increased x_m and decreased T_{sat} . In Fig. 10a, there is an overlap in ΔP_{meas} for $T_{sat} = 50^\circ\text{C}$ and $T_{sat} = 40^\circ\text{C}$. A higher ΔP_{meas} was obtained for $G \leq 300 \text{ kg/m}^2\text{s}$ for $T_{sat} = 50^\circ\text{C}$ when compared with $G \leq 300 \text{ kg/m}^2\text{s}$ for $T_{sat} = 40^\circ\text{C}$. This may likely be due to the variation in the thermo-physical properties of the refrigerant with temperature [20]. In Fig. 10b for $x_m = 0.5$ and $G = 100 \text{ kg/m}^2\text{s}$, the ΔP_{meas} for $T_{sat} = 50^\circ\text{C}$ is higher than that for $T_{sat} = 40^\circ\text{C}$. In Fig. 10c, it is clearly shown that ΔP_{meas} decreases with T_{sat} for all G .

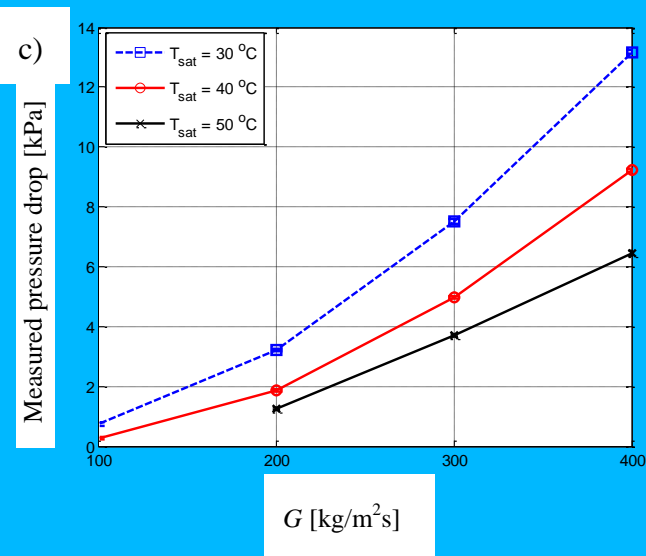
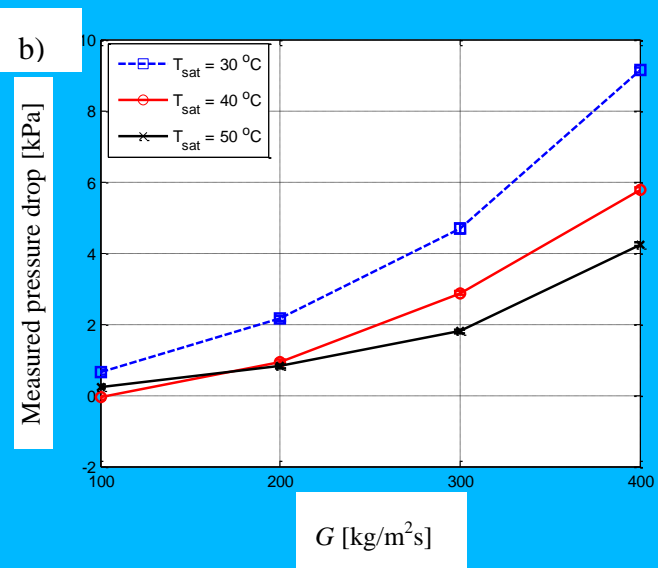
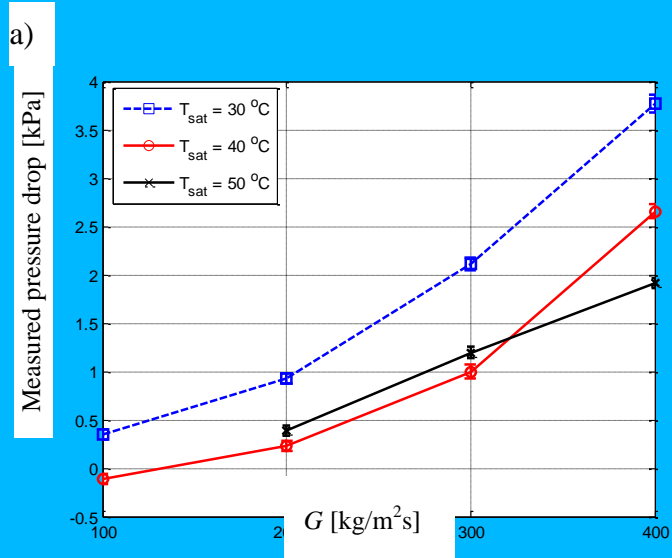


Fig. 10. Effect of G on measured pressure drop for different T_{sat} for $\beta = 0$, a). $x = 0.25$, b). 0.5 and c). 0.75 .

Fig. 11 reveal the behaviour of ΔP_{meas} as a function of x_m at $\beta = 0^\circ$ at different values of T_{sat} for two selected mass flux cases. For $G = 300 \text{ kg/m}^2\text{s}$ Fig. 11a shows the effect of x_m on ΔP_{meas} for $T_{sat} = 30^\circ\text{C}$, 40°C and 50°C . The results reveal that for low x_m ($x_m = 0.1$ and 0.25) ΔP_{meas} for $T_{sat} = 50^\circ\text{C}$ is greater than that for $T_{sat} = 40^\circ\text{C}$ while for $T_{sat} = 30^\circ\text{C}$ is distinctly greater for all x_m . This corresponds to the relative behaviour of the condensation heat transfer coefficient in inclined tube as considered in an earlier study [20]. In that study the effect of T_{sat} on the heat transfer coefficient was attributed to the predominance of gravitational effect at $T_{sat} = 50^\circ\text{C}$ above the shear effect at $T_{sat} = 40^\circ\text{C}$. Fig. 11b shows the same trend for $G = 400 \text{ kg/m}^2\text{s}$ but that the ΔP_{meas} values are greater which distinctly decreases with T_{sat} for all x_m ($0.25 \leq x_m \leq 0.9$).

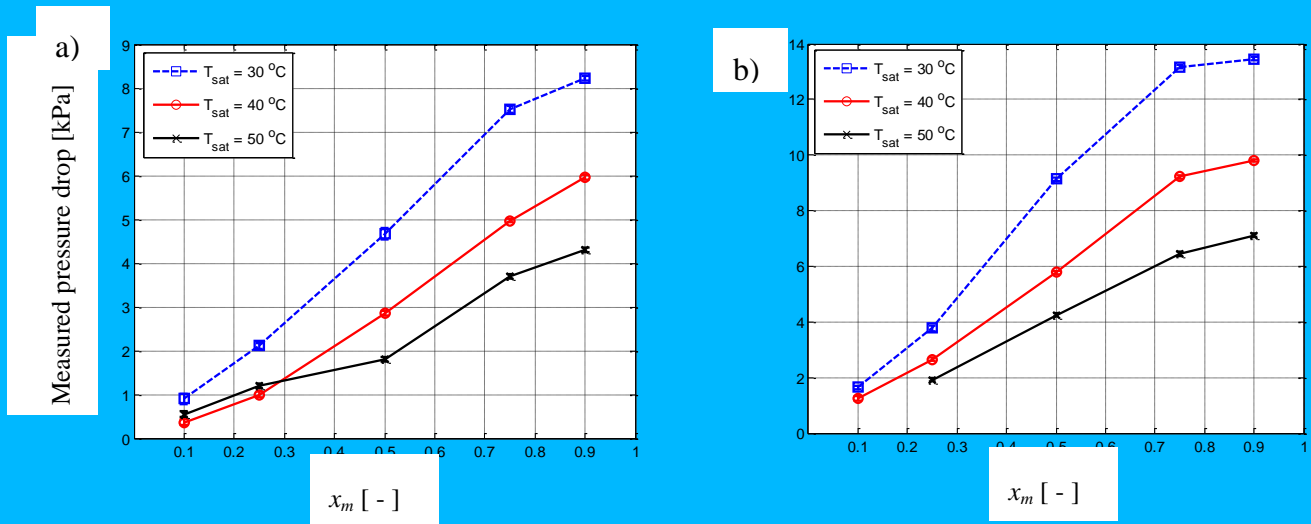


Fig. 11. Effect of mean vapour quality on measured pressure drop for different saturation temperatures for $\beta = 0$ for a) $G = 300 \text{ kg/m}^2\text{s}$ and b) $G = 400 \text{ kg/m}^2\text{s}$.

5. Void Fraction and Frictional Pressure Drop

The effects of inclination angle, vapour quality, mass flux and saturation temperature on the predicted void fraction and the resulting frictional pressure drop are captured in Figs. 12 – 17.

The effects of each of these variables on the predicted void fraction is discussed first

followed by the frictional pressure drop. During the upward inclination ($\beta = 90^\circ$), the void

fraction decreases leading to an increment in the two-phase mixture density as can be seen in eq. (5), hence resulting in an increase in the static/ gravitational pressure drop. Since the momentum pressure drop is small compared to both the static and frictional pressure drop, an increment in the static component will result in a decrease in the frictional pressure drop. The converse is the case for the downward flow when the void fraction increases. This could be explained by referring to the fact that during the downward flow, the action of the gravitational force causes the liquid film on the wall to be thinner, hence resulting in an increased void fraction. The opposite takes place during upward flow. Mixture vapour quality is proportional to the density, so an increase in the vapour quality means a decrease in the liquid hold-up, which will lead to a decrease in the density of the mixture hence the static pressure drop thus an increase in the frictional pressure drop. With respect to the frictional pressure drop, an increase in the mass flux will increase the frictional shear at the wall of the tube causing frictional pressure drop to increase.

Fig. 12 a-c show the effects of inclination and mass flux on the void fraction at $T_{sat} = 30^{\circ}\text{C}$ for mean vapour qualities of 0.25, 0.5 and 0.75. The result show that during the downward flow $-60^{\circ} \leq \beta \leq -90^{\circ}$, the void fraction varies inversely as the mass flux but for $\beta > -60^{\circ}$, the opposite is true. With an increase in the vapor quality, there is an increase in the void fraction. As the inclination angle increases, there is a decrease in the void fraction value from the downward to the upward orientation with the maximum being reached during the vertical upward flow and the minimum being reached in the β range between $+60^{\circ}$ and $+90^{\circ}$. The vertical scatter that is visible in terms of the predicted void fractions is due to the small variations in actual mean vapor quality from one data-point to the next within experimental

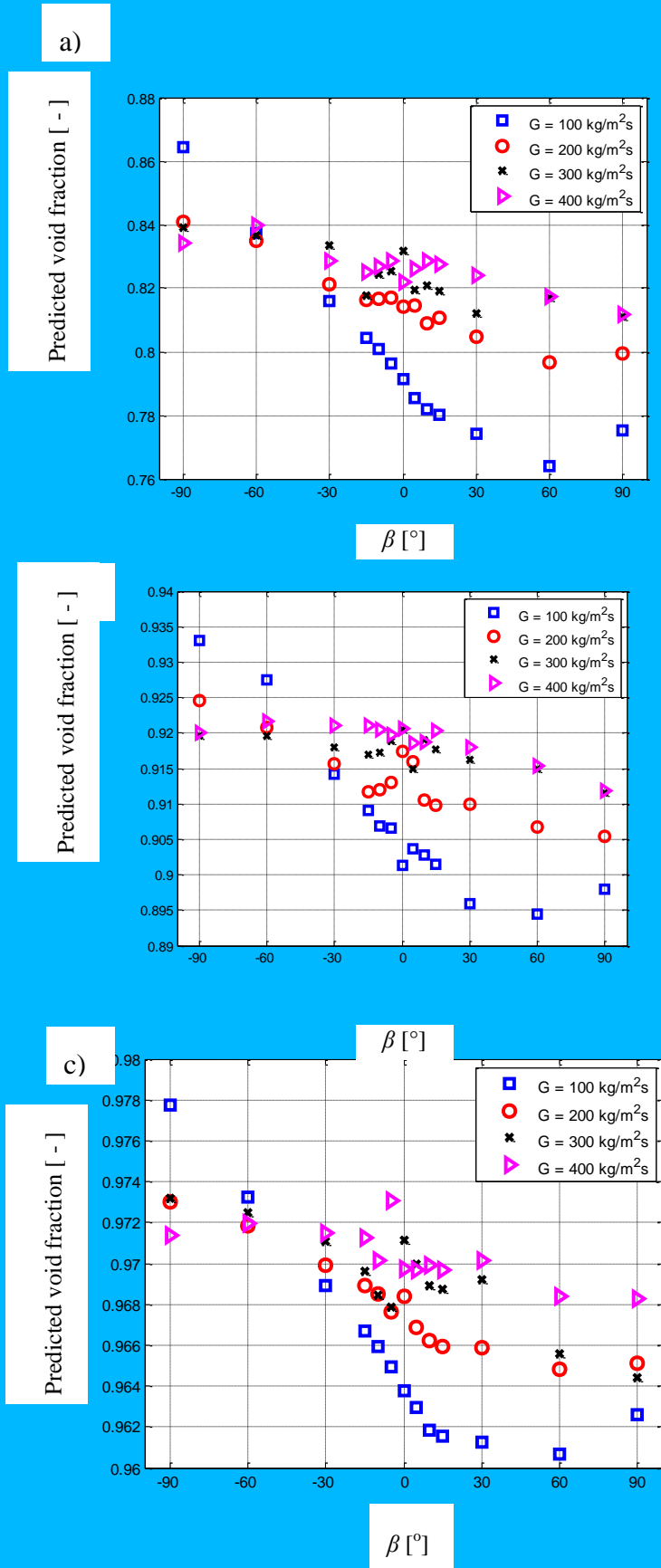


Fig. 12. Effect of inclination angle on void fraction for different mass fluxes for a) $x_m = 0.25$, b) $x_m = 0.5$ and c) $x_m = 0.75$ for $T_{sat} = 30^\circ\text{C}$.

dataset. This was due to the experimental difficulty in maintaining the same quality for all test cases (refer to the band reported in Table 1).

Table 1 Parameters and range

Parameter	Range	Variance
T_{sat} [°C]	30 – 50	± 0.6
G [kg/m ² s]	100 – 400	± 5
x_m	0.1 – 0.9	± 0.01
β [°]	-90° – +90°	± 0.1
Q_{H2O} [W]	250	± 20
ΔP [kPa]	-2 - +12	± 0.05

Fig. 13 shows the variation of void fraction with inclination angle for different quality values. It can be seen that the void fraction increases with quality. At higher mass fluxes it generally decreases from the downward tube orientation to the upward flow, however no generalized profile is observed across all mass flux cases.

Fig. 14 a-c present the variation of void fraction with saturation temperature and inclination angle at a mass flux of 400 kg/m²s for mean vapor qualities of 0.25, 0.5 and 0.75. The results show that the void fraction is inversely proportional to the saturation temperature. For the temperatures considered here there was a variation in the void fraction of up to approximately 0.1 for $x_m = 0.25$ as is seen in Fig. 14 a.

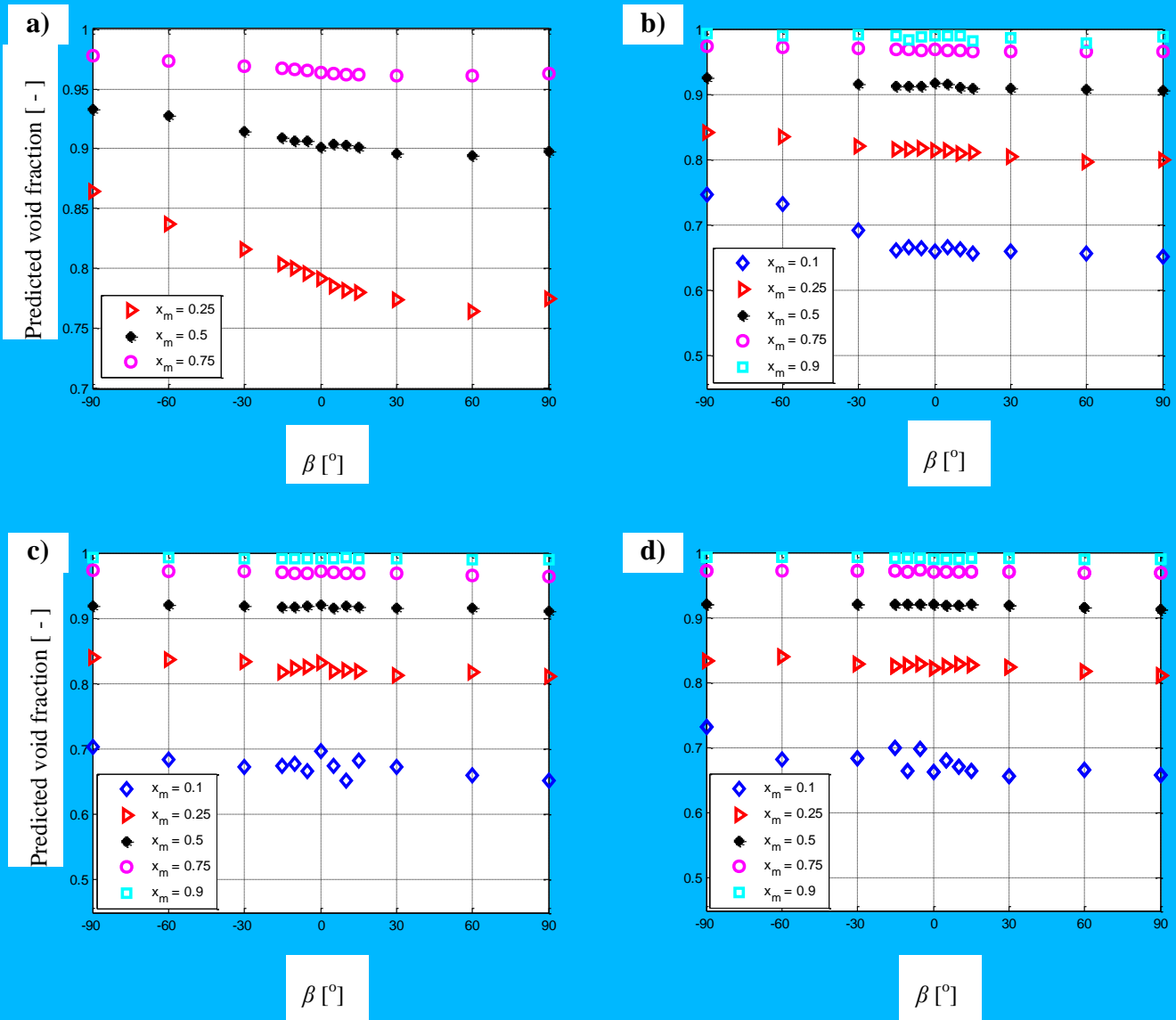


Fig. 13. Effect of inclination angle on void fraction for different vapour qualities for a) $G = 100 \text{ kg/m}^2\text{s}$, b) $G = 200 \text{ kg/m}^2\text{s}$, c) $G = 300 \text{ kg/m}^2\text{s}$, and d) $G = 400 \text{ kg/m}^2\text{s}$ for $T_{sat} = 30^\circ\text{C}$.

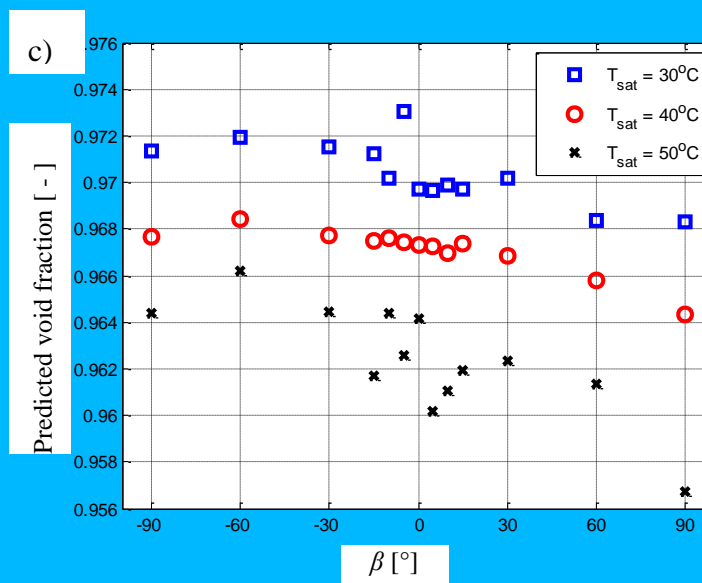
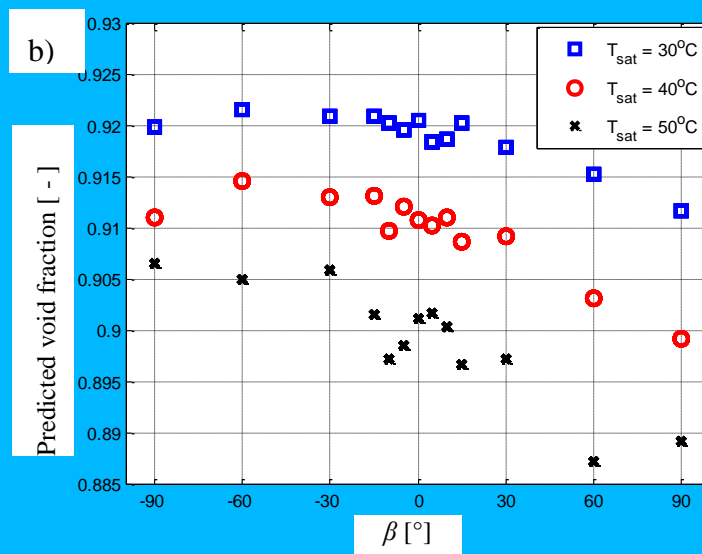
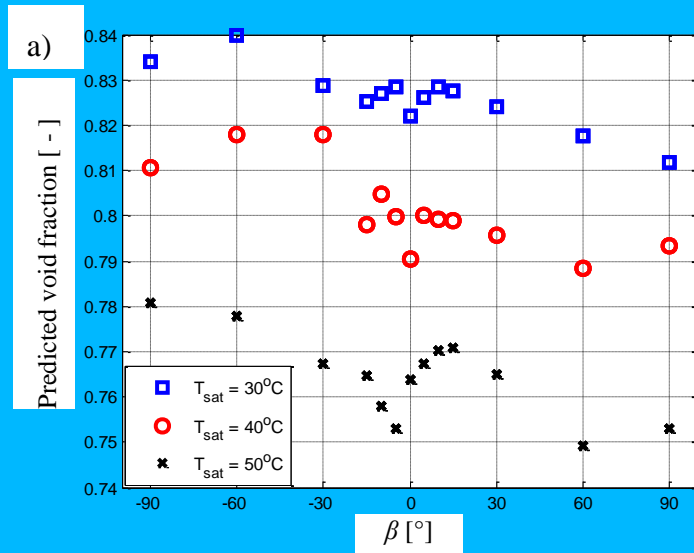


Fig. 14. Effect of inclination angle on void fraction for different saturation temperatures for a) $x_m = 0.25$, b) $x_m = 0.5$ and c) $x_m = 0.75$ for $G = 400 \text{ kg/m}^2\text{s}$.

Figs. 15 and 17 reveal the variation in the calculated frictional pressure drop (based on the predicted void fractions) in terms of the inclination angle and mass flux at $T_{sat} = 30^\circ\text{C}$ for mean vapour qualities of 0.25, 0.5 and 0.75. The results show that the frictional pressure drop increases with either an increase in the mass flux or an increase in the vapour quality. There is however, a decrease with an increase in the saturation temperature. The profile of the frictional pressure drop is unlike that of the total / measured pressure drop that has a maximum during upward flow and a minimum during downward flow. For the frictional pressure drop, the highest value appears to exist during the vertically downward flow while the minimum value appears to exist during horizontal flow (for $x_m = 0.25$) or marginally for vertically upward flow (for $x_m = 0.5$ and 0.75). With an increase in the vapour quality, the effect of inclination on the frictional pressure drop becomes less dominant due to the reduction in the liquid hold-up which impacts the static pressure drop. Fig. 15a particularly reveals that for a vapour quality of 0.25 the frictional pressure drop, irrespective of the mass flux, increases sharply during downward flow and climaxed at $\beta = -90^\circ$, except for $G = 100 \text{ kg/m}^2\text{s}$ where the frictional pressure drop is the highest at $\beta = -60^\circ$ and the minimum was obtained during and close to the horizontal tube orientations.

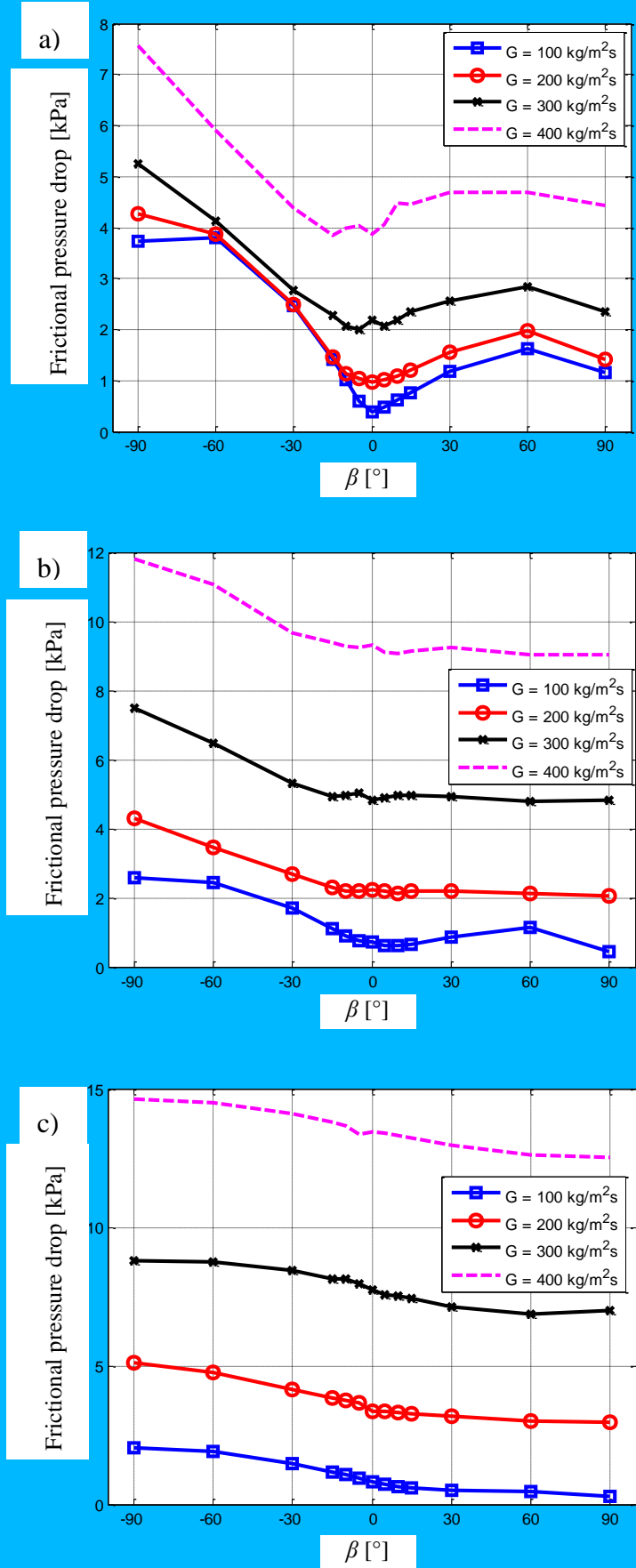


Fig. 15. Effect of inclination angle on frictional pressure drop for different mass fluxes for a) $x_m = 0.25$, b) $x_m =$

Fig. 16 represents the frictional pressure drop as a function of inclination angle and quality for different mass fluxes. Results reveals that for low quality ($x_m = 0.1$ and 0.25) frictional pressure drop decreases monotonically from upward to horizontal tube orientation then increases to a second but lower peak at $\beta = 60^\circ$ and afterwards decreases until the tube orientation is upward vertical. For higher qualities, it decreases from the downward vertical tube orientation to a minimum during upward flow. For $x_m = 0.75$ and 0.9 for $G = 300$ and $400 \text{ kg/m}^2\text{s}$, a waveform profile is observed.

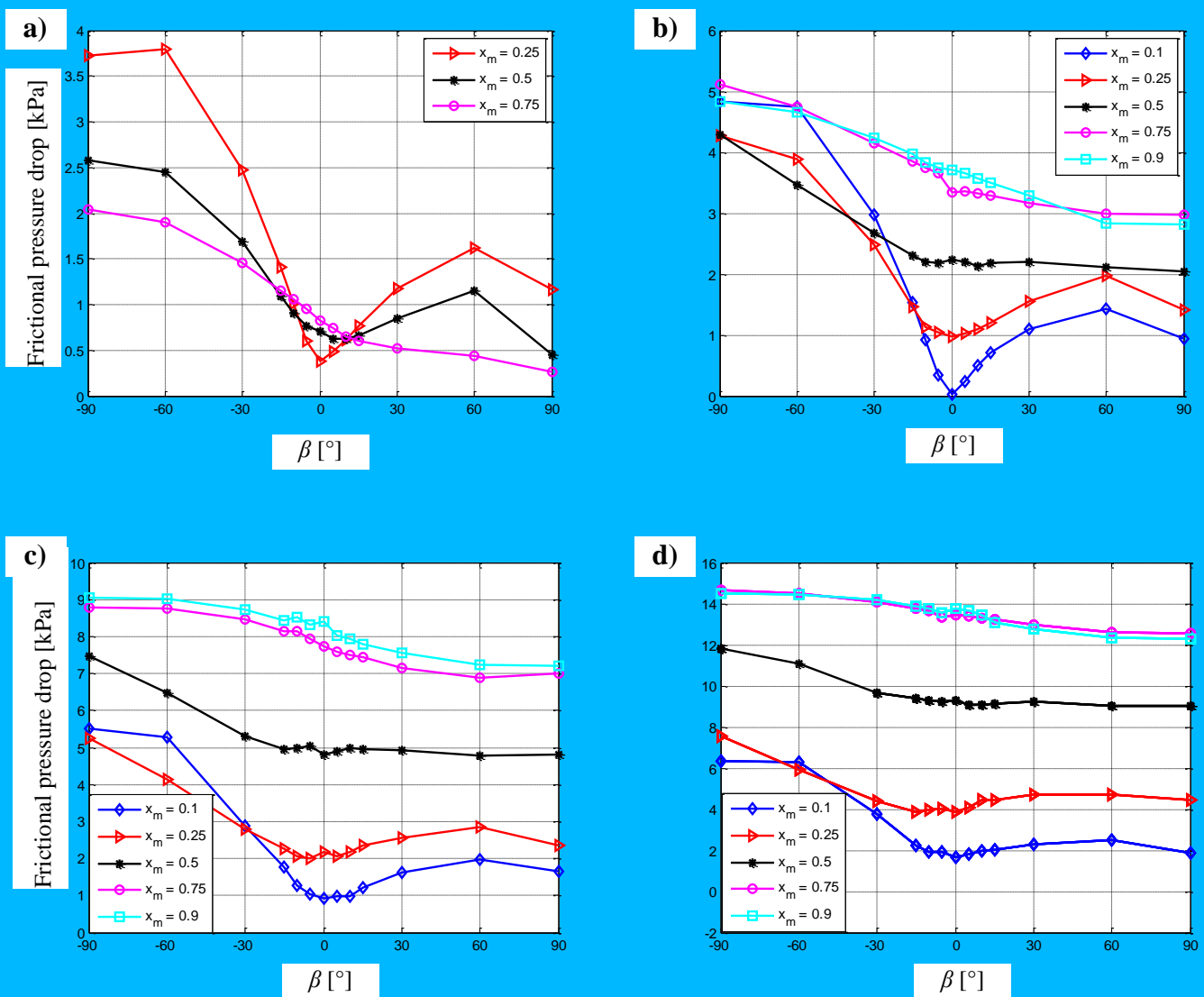


Fig. 16. Effect of inclination angle on frictional pressure drop for different vapour qualities for a) $G = 100 \text{ kg/m}^2\text{s}$, b) $G = 200 \text{ kg/m}^2\text{s}$, c) $G = 300 \text{ kg/m}^2\text{s}$, and d) $G = 400 \text{ kg/m}^2\text{s}$ for $T_{sat} = 30^\circ\text{C}$.

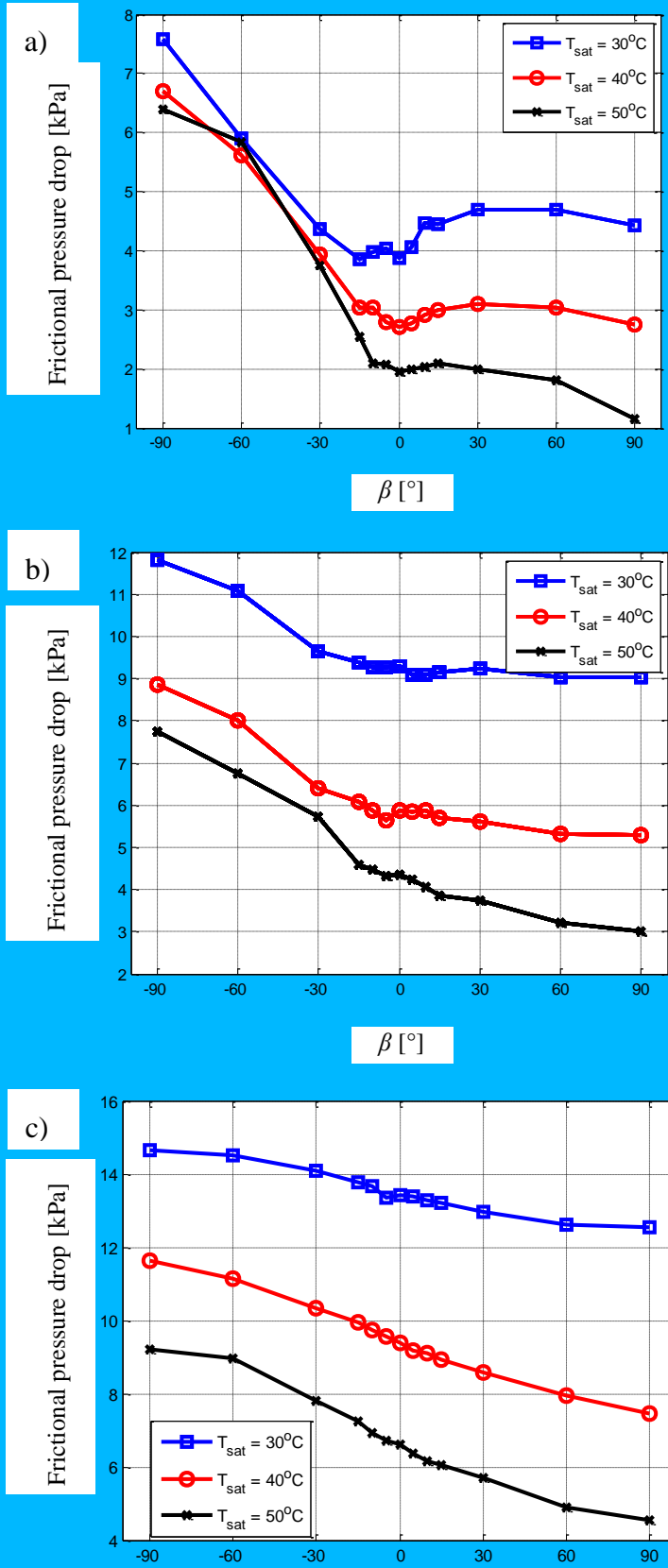


Fig. 17. Effect of inclination angle on frictional pressure drop for different saturation temperatures for a) $x_m = 0.25$, b) $x_m = 0.5$ and c) $x_m = 0.75$ for $G = 400 \text{ kg/m}^2\text{s}$.

Fig. 17 a-c illustrate the effect of inclination and saturation temperature on frictional pressure drop for $G = 400 \text{ kg/m}^2\text{s}$. Results show that the effect of inclination decreases with increase in the vapour quality. This can be attributed to the reduction in the liquid hold-up as vapour quality increases. With saturation temperature, there is a decrease in the frictional pressure drop with increase in the saturation temperature.

6. Conclusion

In the experimental study the specific effects of the inclination angle as well as the saturation temperature on the measured pressure difference and the derived frictional pressure drop for the condensation of R134a were investigated for a smooth inclined tube with an inner diameter of 8.38mm. The following experimental conditions were considered: mean vapour qualities varying between 0.1 and 0.9, saturation temperature varying between 30°C and 50°C, mass fluxes ranging between 100 kg/m²s and 400 kg/m²s, inclination angles ranging between -90° (vertical downward) and +90° (vertical upward) and heat flow rates between 0.23 kW and 0.27 kW. These parameters were found to significantly influence the measured pressure differences as well as the derived frictional pressure drop.

Results show that the inclination angle influences the flow pattern which invariably affects the frictional pressure drop. Highest frictional pressure drops were obtained during vertical downward flow cases, while the lowest frictional pressure drop was obtained either at approximately horizontal tube orientations (for lower vapour qualities) or at vertical upward flow inclinations (for higher vapour qualities). An increase in the saturation temperature leads to a decrease in the frictional pressure drops.

Acknowledgments

The funding obtained from the NRF, TESP, University of Stellenbosch/ University of Pretoria, SANERI/SANEDI, CSIR, EEDSM Hub and NAC is acknowledged and duly appreciated.

References

- [1] A.S. Dalkilic, S. Wongwise, Intensive literature review of condensation inside smooth and enhanced tubes, *Int. J. Heat Mass Transfer* 52 (2009) 3409—3426.
- [2] J.M. Quiben, J.R. Thome, Flow pattern based two-phase frictional pressure drop model for horizontal tubes, Part II: New phenomenological model, *Int. J. Heat and Fluid Flow* 28 (2007) 1060 – 1072.
- [3] S. Lips, J.P. Meyer, Two-phase flow in inclined tubes with specific reference to condensation: a review, *Int. J. Multiphase Flow* 37 (2011) 845-859.
- [4] R.W. Lockhart, R.C. Martinelli, Proposed correlation of data for isothermal two-phase , two-component in pipes, *Chem. Eng. Proce* 45 (1) (1949) 39 – 48.
- [5] D. Chisholm, Pressure gradients due to friction during the flow of evaporating two-phase mixtures in smooth tubes and channels, *Int. J. Heat Mass Transfer* 16 (1973) 347 – 358.
- [6] L. Friedel, Improved friction drop correlations for horizontal and vertical two-phase pipe, European two-phase Flow Group Meeting, paper E2, Ispra, Italy (1979).
- [7] R. Gronnerud, Investigation of liquid hold-up, flow resistance and heat transfer in circulation type of evaporators, Part IV: two-phase flow resistance in boiling refrigerants, Annex 1972 -1, *Bull. De l'Inst. Du Froid* (1979).
- [8] H. Muller- Steinhagen, K. Heck, A simple friction pressure correlation for two-phase flow in pipes, *Chem. Eng. Proce.* 20 (1986) 297 – 308.
- [9] M.W. Spartz, S.F.Y. Motta, An evaluation of options for replacing R22 in medium

- temperature refrigeration systems, *Int. J. Refrigeration* 27 (2004) 475 – 483.
- [10] A. Cavallini, D. Del Col, L. Doretti, G.A Longo, L. Rossetto, Enhance in-tube heat transfer with refrigerant, 20th Int. Congress of Refrigeration, IIR/IIF (1999) Sydney.
- [11] J.Y. Choi, M.A. Kedzierski, P.A. Domanski, A generalized pressure drop correlation for evaporation and condensation of alternative refrigerant in smooth and micro-fin tubes, NISTIR (1999) 6333.
- [12] M. Ghodbane, An investigation of R152a and hydrocarbon refrigerants in mobile air conditioning, SAE Tech. Pap. Ser. (Soc. Automot. Eng.) (1999) 17.
- [13] W.W. Akers, H.F. Rosson, Condensation inside horizontal tubes, *Progr. Symp. Ser.* 56 (30) (1960).
- [14] A.E. Dukler, Gas liquid flow in pipelines, AGA/API Res. (1969).
- [15] J. Bandel, Druckcerlust und warmeugang bei der verdampfung siedender kaltemittel im durchstromten waagerechten rohr. Ph.D. thesis, University of Karlsruhe, 1973.
- [16] D.R.H. Beattie, Two-phase flow structure and mixing length theory, *Nucl. Eng. Des.* 21 (1972) 46 – 64.
- [17] J. Hart, P.J. Hamersma, J.M.H. Fortuin, Correlations predicting frictional pressure drop and liquid hold-up during horizontal gas-liquid pipe flow with a small liquid hold-up, *Int. J. Multiphase Flow* 15 (6) (1989) 947 – 964.
- [18] C. Tribbe, H.M. Muller- Steinhagen, An evaluation of the performance of phenomenological models for predicting pressure gradient during gas-liquid flow in horizontal pipelines, *Int. J. Multiphase Flow* 26 (2000) 1019 – 1036.
- [19] M.B. Ould-Didi, N. Kattan, J.R. Thome, Prediction of two-phase pressure gradient of refrigerants in horizontal tubes, *Int. J. Refrigeration* 25 (2002) 935 – 947.
- [20] J.P. Meyer, J. Dirker , A.O. Adelaja, Condensation heat transfer in smooth inclined tubes for R134a at different saturation temperatures, *Int. J. Heat and Mass Transfer* 70 (2014) 515-

525.

- [21] P. A. Patil, S.N. Sapali, Condensation pressure drop of HFC-134a and R-404A in a smooth and micro-fin U-tube, *Exp. Therm. Fluid Sci.* 35 (2011) 234–242.
- [22] Y. J. Kim, J. Jang, P. S. Hrnjak, M. S. Kim, Adiabatic horizontal and vertical pressure drop of carbon dioxide inside smooth and microfin tubes at low temperatures, *ASME Journal of Heat Transfer*, NOVEMBER 2008, Vol. 130 / 111001-1.
- [23] A. Cavallini, G. Censi, D. Del Col, L. Doretti, G.A. Longo, L. Rossetto, Experimental investigation on condensation heat transfer and pressure drop of new HFC refrigerants (R134a, R125, R32, R410A, R236ea) in a horizontal smooth tube, *Int. J. Refrigeration* 24 (2001) 73-87.
- [24] S.M. Bhagwat, and A.J. Ghajar, A flow pattern independent drift flow model based void fraction correlation for a wide range of gas-liquid two-phase flow, *International Journal of Multiphase Flow*, Vol. 59, 2014, pp. 188-205.
- [25] S. Lips, J.P. Meyer, Experimental study of convective condensation in an inclined smooth tube. Part II: Inclination effect on pressure drops and void fractions, *Int. J. Heat and Mass Transfer* 55 (2012) 405 - 412.
- [26] A.O. Adelaja, J. Dirker, J.P. Meyer, Condensing heat transfer coefficients for R134a at different saturation temperatures in inclined tubes, *Proceedings of the ASME2013 Summer Heat Transfer Conference* (HT 2013 - 17375), Minneapolis, MN, USA, 2013, pp. 1- 9.
- [27] A.O. Adelaja, J. Dirker, J.P. Meyer, Experimental studies of condensation heat transfer in an inclined microfin tube, *Proceedings of the 15th International Heat Transfer Conference, (IHTC-15)*, Kyoto, 2014, pp. 1- 14.
- [28] A.O. Adelaja, D.R.E Ewim, J. Dirker, J.P. Meyer, Experimental investigation on pressure drop and friction factor in tubes at different inclination angles during the condensation of R134a, *Proceedings of the 15th International Heat Transfer Conference, (IHTC-15)*, Kyoto,

- 2014, pp. 1- 14.
- [29] REFPROP., NIST Thermodynamic properties of refrigerants and refrigerant mixtures (REFPROP), version 8.0, NIST Standard Reference Database 23, National Institute of Standards and Technology, Gaithersbury, MD, 2005.
- [30] A.J. Ghajar, A.J, S.M Bhagwat, Effect of void fraction and two-phase dynamic viscosity models on prediction of hydrostatic and frictional pressure drop in vertical upward gas-liquid two-phase flow, *Heat Transfer Engineering*, Vol. 34, 2013, pp 1044-1059.
- [31] A.J. Ghajar, C.C Tang, Void fraction and flow pattern of two phase flow in upward, downward and horizontal pipes, *Advanced Multiphase Flow Heat Transfer*, Chapter 4, 2012, pp 175-201.
- [32] M. Kaji, B.J. Azzopardi, The effect of pipe diameter on the structure of gas-liquid flow in vertical pipes, *International Journal of Multiphase Flow*, Vol. 36, 2010, pp. 303 – 313.
- [33] K. Mishima, T. Hibiki, Some characteristics of air-water in two phase flow in small diameter vertical tubes, *International Journal of Multiphase Flow*, Vo. 22, 1996, pp. 703-712.
- [34] M. Shoukri, I. Hassan, I. Gerges, Two-phase bubbly flow structure in large diameter vertical pipe, *The Canadian Journal of Chemical Engineering*, Vol. 81, 2003, 205-211.
- [35] S.P Olivier, J.P. Meyer, M. De Paepe and K. De Kerpel, The influencer of inclination angle on void fraction and heat transfer during condensation inside a smooth tube, *International Journal of Multiphase Flow*, manuscript number IJMF-D-15-00209R1, accepted on 13 October 2015.
- [36] R. J. Moffat, Describing the uncertainties in experimental results, *Exp. Therm Fluid Sci.* 1 (1988) 3 – 17.
- [37] W. Zhang, T. Hibiki, K. Mishima, Correlations of two-phase frictional pressure drop and void fraction in mini-channel, *Int. J. Heat Mass Transfer* 53, 2010, 453 – 465.
- [38] M. Zangana, G.P. van der Muelen, B.J. Azzopardi, The effect of gas and liquid

velocities on frictional pressure drop in two phase flow for large diameter vertical pipe, Proceedings of 7th International Conference on Multiphase Flow ICMF 2010, Tampa, Florida, USA May 30 – June 4, 2010.

[39] H Liu, C.O. Vandu, R. Krishna, Hydrodynamics of Taylor flow in vertical capillaries: flow regimes, bubble rise velocity, liquid slug length, and pressure drop, *Ind. Eng. Chem. Res.* 44, 2005, 4884 – 4897.

[40] P.L. Spedding, E. Benard, Gas-liquid two phase flow through a vertical 90° elbow bend, *Experimental Thermal Fluid Science* 31, 2007, 761 – 769.

[41] K. Cornwell, P.A. Kew, Boiling in small parallel channel, Proc. CEC Conference on Energy Efficiency in Process Technology, Athens, Greece, October 1992, Elsevier Applied Sciences, 624 – 638.

[42] D.J. Nicklin, Two-phase bubble flow, *Chem. Eng. Sci.* 17, 1962, 693.

[43] S. Kandlikar, Two-phase flow patterns, pressure drop, and heat transfer during boiling in Minichannel flow passages of compact evaporators, *Heat Transfer Engineering* 23, 2002, 5 – 23.

[44] F.A. Ribas, C. J. Deschamps, Friction factor under transient flow condition, *Int. compressor Engineering Conference*, paper no. 1665, 2004, C097, 1 - 8.